Biosci. Rep. (2011) / **31** / 371–379 (Printed in Great Britain) / doi 10.1042/BSR20100123

online data multimedia

Original Paper

Bioscience Reports

# IQ-motif selectivity in human IQGAP2 and IQGAP3: binding of calmodulin and myosin essential light chain

Erwan ATCHESON, Elaine HAMILTON[1], Sevvel PATHMANATHAN[2], Brett GREER, Pat HARRIOTT and David J. TIMSON[3]

School of Biological Sciences, Queen's University Belfast, Medical Biology Centre, 97 Lisburn Road, Belfast BT9 7BL, U.K.

**Synopsis**

The IQGAP [IQ-motif-containing GAP (GTPase-activating protein)] family members are eukaryotic proteins that act at the interface between cellular signalling and the cytoskeleton. As such they collect numerous inputs from a variety of signalling pathways. A key binding partner is the calcium-sensing protein CaM (calmodulin). This protein binds mainly through a series of IQ-motifs which are located towards the middle of the primary sequence of the IQGAPs. In some IQGAPs, these motifs also provide binding sites for CaM-like proteins such as myosin essential light chain and S100B. Using synthetic peptides and native gel electrophoresis, the binding properties of the IQ-motifs from human IQGAP2 and IQGAP3 have been mapped. The second and third IQ-motifs in IQGAP2 and all four of the IQ-motifs of IQGAP3 interacted with CaM in the presence of calcium ions. However, there were differences in the type of interaction: while some IQ-motifs were able to form complexes with CaM which were stable under the conditions of the experiment, others formed more transient interactions. The first IQ-motifs from IQGAP2 and IQGAP3 formed transient interactions with CaM in the absence of calcium and the first motif from IQGAP3 formed a transient interaction with the myosin essential light chain Mlc1sa. None of these IQ-motifs interacted with S100B. Molecular modelling suggested that all of the IQ-motifs, except the first one from IQGAP2 formed $\alpha$-helices in solution. These results extend our knowledge of the selectivity of IQ-motifs for CaM and related proteins.

*Key words:* $\alpha$-helical peptide, calcium-dependent interaction, IQ-motif-containing GTPase-activating protein (IQGAP), IQ-motif, myosin essential light chain, native gel electrophoresis

www.bioscirep.org

Bioscience Reports

## INTRODUCTION

The IQ-motif is present in a wide variety of proteins that bind to CaM (calmodulin) and structurally related proteins [1–3]. The consensus sequence for the motif is generally accepted to be IQXXXRGXXXR, where X is any amino acid [2]. Nevertheless the motif shows considerable variation, even in the five consensus residues. Sequences containing the motif are usually $\alpha$-helical in conformation and CaM (and similar proteins) bind to this motif by partially wrapping around this $\alpha$-helix. Multiple IQ-motifs are present in most members of the myosin superfamily where they mediate interactions between CaM and various types of myosin light chain [4,5].

CaM is a widely distributed intracellular sensor of calcium ions. It binds to a wide variety of cellular targets in order to transduce calcium-based signals. A key group of targets in signalling to the cytoskeleton are the IQGAP [IQ-motif-containing GAP (GTPase-activating protein)] family of proteins [6]. These relatively large proteins (150–180 kDa) sit at the interface between cellular signalling and cytoskeletal reorganization [7–12]. They bind to a variety of signalling molecules (including kinases, growth factor receptors and small GTPases [11]), integrate the information received from them and pass it on to the cytoskeleton. This is achieved by direct interaction with actin [13], by interaction with actin-organizing proteins such as N-WASP (neuronal Wiskott–Aldrich syndrome protein) [14] and by regulation of microtubule-organizing proteins such as CLIP-170 (cytoplasmic

**Abbreviations used:** APC, adenomatous polyposis coli; CaM, calmodulin; CDC42, cell division cycle 42; DTT, dithiothreitol; Fmoc, fluoren-9-ylmethoxycarbonyl; GAP, GTPase-activating protein; IQGAP, IQ-motif-containing GTPase-activating protein; LB, Luria–Bertani; TFA, trifluoroacetic acid.

[1]Present address: Belfast Metropolitan College, Castlereagh Campus, Montgomery Road, Belfast BT6 9JD, U.K.

[2]Present address: Department of Botany, The University of Jaffna, Jaffna, Sri Lanka.

[3]To whom correspondence should be addressed (email d.timson@qub.ac.uk).

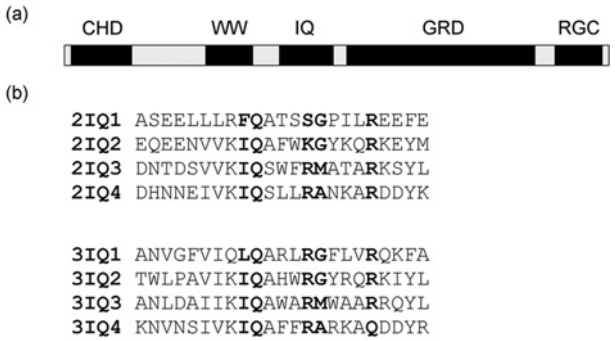


**Figure 1 The general primary structure of IQGAP family members and the peptides used in the present paper**

(a) A schematic diagram of the motifs found in IQGAP family proteins (not to scale). CHD, calponin homology domain; WW, WW domain; IQ, IQ-motif containing region; GRD, GAP-related domain; RGC, Ras-GAP C-terminal domain. (b) The peptide sequences used in the present study. Sequences derived from IQGAP2 are designated 2IQ1, 2IQ2, 2IQ3 and 2IQ4 in the order they appear in the primary sequence. Similarly, those derived from IQGAP3 are designated 3IQ1, 3IQ2, 3IQ3 and 3IQ4. The diagnostic, commonly conserved residues of IQ-motifs are highlighted in bold. Note that, as seen here, there is considerable variation in many IQ-motifs, including at these key residues.

linker protein-170) and the APC (adenomatous polyposis coli) protein [15,16].

Members of the IQGAP family are multi-domain proteins (Figure 1a). At the N-terminus is the calponin homology domain that interacts with actin (and may also bind to CaM) [13,17–20]. The C-terminal GAP-related domain interacts with, and inhibits, the small GTPases CDC42 (cell division cycle 42) and Rac1 [6,19,21–26]. The C-terminal region also interacts with CLIP-170 and APC [15,16]. A number of IQ-motifs are located approximately in the middle of the primary sequence. The exact number varies according to isoform and species. In the three human isoforms, IQGAP1, IQGAP2 and IQGAP3, there are four, except in an alternatively spliced testicular form of IQGAP2 which has only three [6,12,22,27,28]. The situation in the budding yeast (*Saccharomyces cerevisiae*) IQGAP protein, Iqg1p, is more complicated. Here, difficulty in identifying IQ-motifs has lead to different numbers of IQ-motifs being proposed. There appear to be at least eight, but some authors suggest that there may be as few as five or as many as 11 [29–31].

The IQ-motifs of the IQGAP family interact with CaM [22,32]. However, it appears that not all of them interact under the same conditions. For example, some IQ-motifs in human IQGAP1 are occupied with CaM only in the presence of calcium ions, whereas others are able to interact regardless of the calcium concentration [32,33]. Some IQGAPs, including human IQGAP1, *S. cerevisiae* Iqg1p and *Schizosaccharomyces pombe* Rng2p interact with myosin essential light chains [24,30,34–36]. The physiological significance of this interaction in humans is unknown, but in yeasts it is required for the successful completion of cytokinesis [20,30,31,37–43]. Human IQGAP1 also interacts, through its IQ-motifs, with S100B [35,44]. This interaction is important in the cytoskeleton-mediated rearrangement of cell membranes [44].

In order to understand the IQGAPs' overall function as signal integrators, it is necessary to understand what binds, where it binds and under what conditions it binds. Although considerable work has been done to understand the interactions of human IQGAP1 with CaM (e.g. [9,32,33]), relatively little work has been done on IQGAP2 and IQGAP3. Here, the interaction of IQ-motifs in these two proteins with CaM and myosin essential light chain was mapped using synthetic peptides corresponding to the IQ-motifs (Figure 1b) and native gel electrophoresis.

## MATERIALS AND METHODS

### Protein expression and purification

The myosin essential light chain, Mlc1sa and S100B were prepared as previously described [35]. The coding sequence for human CaM was amplified by PCR from the IMAGE clone (ID 2821489) [45] using primers that incorporated NcoI and XhoI restriction enzyme sites at the 5′ and 3′ ends respectively. This sequence was cloned into the respective sites in pET-21d (Novagen) such that the coding sequence was in frame with the $His_6$ tag-encoding sequence in the vector. The sequence of the coding sequence was verified (MWG Biotech). Thus the expressed protein incorporated the amino acid residues LEHHHHHH at the C-terminus in addition to the full-length sequence of human CaM. *Escherichia coli* Rosetta (DE3) cells were transformed with this expression vector. A single colony was picked and grown, overnight, shaking at 30°C in LB (Luria–Bertani) broth supplemented with 100 $\mu$g/ml ampicillin and 100 $\mu$g/ml chloramphenicol. This culture was diluted into 1 litre of LB broth (supplemented with 100 $\mu$g/ml ampicillin and 100 $\mu$g/ml chloramphenicol) and grown, shaking, at 30°C until the $D_{600}$ reached 0.6–1.0 (approx. 3–4 h). The culture was then induced by addition of IPTG (isopropyl $\beta$-D-thiogalactoside) to a final concentration of 2 mM and grown for a further 3 h. The cells were harvested by centrifugation (4000 ***g*** for 15 min), resuspended in buffer R [50 mM Hepes-OH, pH 7.5, 150 mM sodium chloride and 10 % (v/v) glycerol] and stored at − 80°C until required.

Cell resuspensions were thawed and then sonicated on ice (three pulses of 100 W for 30 s with 30–60 s gaps in between for cooling) to release the proteins. The insoluble matter was pelleted by centrifugation (22 000 ***g*** for 15 min). The supernatant was made of 0.5 mM in calcium chloride and then immediately applied to a phenyl-Sepharose column (3 ml; Sigma), which had been previously equilibrated in 50 mM Hepes-OH, pH 7.5, 5 mM calcium chloride, 100 mM sodium chloride and 0.5 mM DTT (dithiothreitol). The protein was allowed to flow through under gravity. The column was washed with 20 ml of 50 mM Hepes-OH, pH 7.5, 0.1 mM calcium chloride, 100 mM sodium chloride followed by 50 mM Hepes-OH, pH 7.5, 0.1 mM calcium chloride and 500 mM sodium chloride. CaM was eluted with three 2 ml washes with 50 mM Hepes-OH, pH 7.5, 1 mM EGTA. CaM-containing fractions were identified by SDS/PAGE (15 % gel) and dialysed against buffer R supplemented with 2 mM DTT. Protein concentrations were determined using the method of Bradford

[46] with BSA as a standard. Proteins were stored in 50–100 $\mu$l aliquots at $-80^{\circ}$C.

### Peptide synthesis

Peptides corresponding to the IQ-motifs from IQGAP2 were designated 2IQ1, 2IQ2, 2IQ3 and 2IQ4 in the order in which they occur in the primary sequence. Similar nomenclature was used for those corresponding to IQGAP3 (Figure 1b). Peptides were synthesized by solid-phase peptide synthesis using standard Fmoc (fluoren-9-ylmethoxycarbonyl) chemistry [47] at a scale of 20 $\mu$mol using a 433A Peptide Synthesizer (Applera). Each peptide was synthesized on a Rink Amide MBHA resin (Merck Biosciences) to produce a free amide upon cleavage and was then capped at the N-terminus using acetic anhydride. Peptides were elongated using 2-(1H-7-azabenzotriazol-1-yl)-1,1,3,3-tetramethyluronium hexafluorophosphate methanaminium (HATU) and DIEA (*N*,*N*-diisopropylethylamine) as coupling agents and 5-fold molar excesses of each *N*-$\alpha$-Fmoc-protected amino acid (Merck). The synthesized peptides were cleaved from the resin by stirring for 2.5 h at 20°C in TFA (trifluoroacetic acid)/ethanedithiol/triisopropylsilane/water (97:1:1:1, by vol.), then separated from the resin by filtration under pressure using a glass-sintered funnel and precipitated with diethyl ether several times. This pellet was then resuspended in water and lyophilized. Peptide purity was then analysed by reverse-phase HPLC using a Gemini-$C_{18}$ column of dimensions 250 mm×4.6 mm (Phenomenex) and eluted with a linear gradient of 0.05 % TFA in acetonitrile and 0.05 % TFA in water from a ratio of 1:49 to 3:2, at a flow rate of 1 ml/min with UV detection at a wavelength of 214 nm. The molecular masses of the peptides were verified using a Finnigan LCQ Ion Trap Mass Spectrometer (Thermo Scientific).

### Native gel electrophoresis

Protein–peptide interactions were detected by native gel electrophoresis. Reaction mixes (35 $\mu$l) contained protein at a fixed concentration of 35 $\mu$M and peptide concentrations varying from 18 to 350 $\mu$M. These mixes (together with protein-only and peptide-only controls) were incubated at 22°C for 1 h, mixed with 15 $\mu$l of loading buffer [125 mM Tris/HCl, pH 6.8, 20 % (v/v) glycerol, 1 % (w/v) DTT and 0.002 % (w/v) Bromophenol Blue] and then loaded on to native gels (20 cm×20 cm; 1 mm thick). The gels comprised a stacking gel [5 % (w/v) polyacrylamide and 125 mM Tris/HCl, pH 6.8] and a separating gel of 15 % (w/v) polyacrylamide in 375 mM Tris/HCl (pH 8.8). The gels were electrophoresed at 15–30 mA (constant current) for 4.5–8 h with 25 mM Tris/HCl (pH 8.8) and 250 mM glycine as the running buffer. On completion of electrophoresis, the gels were stained in 0.25 % (w/v) Coomassie Brilliant Blue R250 (Sigma) dissolved in 10 % (v/v) acetic acid/45 % (v/v) ethanol and destained fully in 5 % (v/v) ethanol; 7.5 % (v/v) acetic acid. Gels were imaged using a ChemiDoc XRS gel documentation system (Bio-Rad).

Where discrete shifts were detected, the fraction bound was estimated by densitometry using Quantity One software (Bio-Rad). Care was taken to ensure that no saturated pixels were present in the images used. The background density per unit area was estimated by selecting three to five random areas away from the bands. Since the bands were not of equal sizes, areas containing all of each of the bands were selected by eye and the density estimated. These densities were then normalized by dividing the area of the box and corrected by subtracting the mean background density per unit area. The fraction bound ($Y$) was then estimated by dividing the corrected, normalized intensity of the upper band (the protein–peptide complex) by the sum of the corrected, normalized intensities of the upper and lower (free protein) bands. The mean values of $Y$ from three independent experiments were plotted against peptide concentration. The apparent dissociation constant ($K_{d,app}$) was estimated by non-linear curve fitting [48] (as implemented in GraphPad Prism 3.0, GraphPad Software, CA, U.S.A.) to the equation $Y = Y_{max}[\text{peptide}]/K_{d,app} + [\text{peptide}]$, where $Y_{max}$ is the maximum (limiting) value of $Y$.

### Peptide modelling

The peptide sequences were submitted to the Phyre online molecular modelling server (http://www.sbg.bio.ic.ac.uk/~phyre/) [49]. Since the peptides were shorter than the minimum length required by this program, they were extended with polyalanine. None of these additional alanine residues appeared in the final models. The highest ranked model was then computationally solvated and the energy of the resulting complex minimized using YASARA (http://www.yasara.org/minimizationserver.htm) [50]. The PDB files of the final, minimized and solvated models are provided as supplementary data (available at http://www.bioscirep.org/bsr/031/bsr0310371add.htm).

## RESULTS

### Expression and purification of human CaM in *E. coli*

Initial attempts to purify recombinant human CaM from extracts of *E. coli* cells using nickel–agarose resin to capture the C-terminal $His_6$ tag were not successful. Typically the purifications resulted in two to three other proteins at comparable concentrations to CaM (results not shown). However, purification based on using phenyl-Sepharose, based on the method of Gopalakrishna and Anderson [51] was successful. This resulted in a single major band (>90 % of eluted material) on SDS/PAGE (Supplementary Figure S1 available at http://www.bioscirep.org/bsr/031/bsr0310371add.htm) and yields of approx. 5 mg of CaM per litre of bacterial culture.

### Interaction of IQ-motifs from human IQGAP2 and IQGAP3 with CaM

Initial screens for interaction with CaM (35 $\mu$M) were carried out with all eight peptides (350 $\mu$M) in the presence (5 mM calcium chloride) and absence (5 mM EGTA) of calcium ions. These

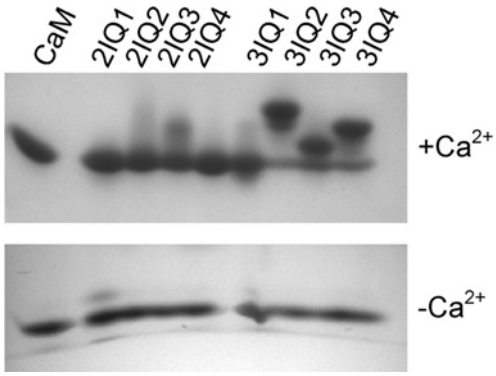


**Figure 2 Interactions of IQ-motif peptides (350 $\mu$M) from IQGAP2 and IQGAP3 with CaM (35 $\mu$M) in the presence and absence of calcium ions under the conditions of native gel electrophoresis (see the Materials and methods section)**
These results are representative of three independent experiments.

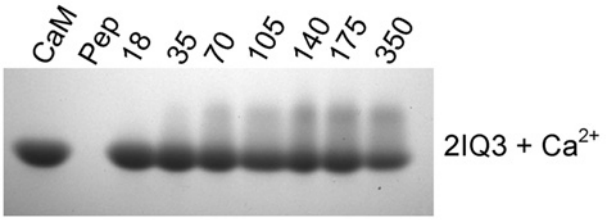


**Figure 3 Interaction of the third IQ-motif from IQGAP2 with CaM (35 $\mu$M) in the presence of calcium ions**
The interaction shows a clear dependence of shift on peptide concentration. The numbers above the gel indicate the peptide concentration in $\mu$M. CaM represents the calmodulin-only (35 $\mu$M) control and Pep the peptide-only (350 $\mu$M) control. These results are representative of three independent experiments.

revealed that 2IQ2, 2IQ3, 3IQ1, 3IQ2, 3IQ3 and 3IQ4 interacted in the presence of calcium ions under these conditions (Figure 2). The nature of these interactions was not identical. In some cases (2IQ3, 3IQ2, 3IQ3 and 3IQ4) discrete shifts were observed, suggesting a relatively long-lived stable complex is formed. Other IQ-motifs (2IQ2, 3IQ1) caused a blurring of the CaM band, suggesting that a more transient interaction has occurred. Fewer interactions were observed in the absence of calcium ions. Under these conditions, only 2IQ1 and perhaps 3IQ1 appeared to interact (Figure 2).

Where discrete, stable interactions were observed, these were quantified by titration of the peptide concentration and densitometric estimation of the fraction bound. It should be noted that the apparent dissociation constants obtained by this method will be highly influenced on the conditions of the experiment and are unlikely to be accurate estimates of the *in vivo*, cellular affinities. Nevertheless, they do enable the ranking of the affinities of interaction. It was not possible to quantify the interaction of 2IQ3 with CaM in the presence of calcium ions. Although this peptide caused a clear, dose-dependent shift in the migration of CaM this shift was a mixture of discrete bands and blurring (Figure 3). This suggests that this IQ-motif's behaviour is intermediate between those which bind stably and those which are in more rapid exchange. However, the interactions between CaM and 3IQ2, 3IQ3 and 3IQ4 in the presence of calcium could be quantified, revealing that the affinity is greatest for 3IQ2, followed by 3IQ4 and then 3IQ3 (Figure 4 and Table 1).

**Table 1 Apparent binding constants ($K_{d,app}$) for the interactions between IQ-motifs from human IQGAP3 and CaM in the presence of calcium ions**
These values were determined from native gel electrophoresis as described in the Materials and methods section and are shown $\pm$ S.E.M. derived from the curve fitting. nd, not determined.

| IQ-motif | $K_{d,app}$ ($\mu$M) |
|---|---|
| 3IQ1 | nd |
| 3IQ2 | 27 $\pm$ 4 |
| 3IQ3 | 76 $\pm$ 18 |
| 3IQ4 | 65 $\pm$ 12 |

## Interaction of IQ-motifs from human IQGAP2 and IQGAP3 with myosin essential light chain and S100B

Previous work has demonstrated that IQGAP1 interacts, through its first IQ-motif, with the myosin essential light chain Mlc1sa and, through its first and second IQ-motifs, with S100B [35]. Increasing concentrations of 3IQ1 caused blurring of the Mlc1sa band in a native gel shift assay (Figure 5). The peptides 3IQ2 and 3IQ3 caused some loss of intensity of the Mlc1sa band at high concentrations without the appearance of a detectable additional band. No interactions were detected between Mlc1sa and 3IQ4 or with any of the IQ-motifs from IQGAP2 (Figure 5). Furthermore, no interactions between S100B and any of the IQ-motifs were detected (results not shown).

## Structural models of IQ-motifs from human IQGAP2 and IQGAP3

To help understand the differences in affinity between the various IQ-motifs and CaM, structural models were constructed. As expected, the majority of the motifs are predicted to adopt an $\alpha$-helical conformation in solution. The one exception is 2IQ1, which adopts a disordered, random coil conformation (Figure 6). In addition, the model for 3IQ3 only contains approximately half the residues in an $\alpha$-helical conformation. The remainder were not modelled by Phyre. Therefore, it is possible that this motif also has some disordered residues in solution. These are modelled structures and so should be treated with some caution. In particular, it is likely that the conformation of the motifs alters on interaction with targets. Nevertheless, these models suggest that the majority of the IQ-motifs that interact with CaM will do so in a manner similar to that observed in myosins (e.g. [4]).

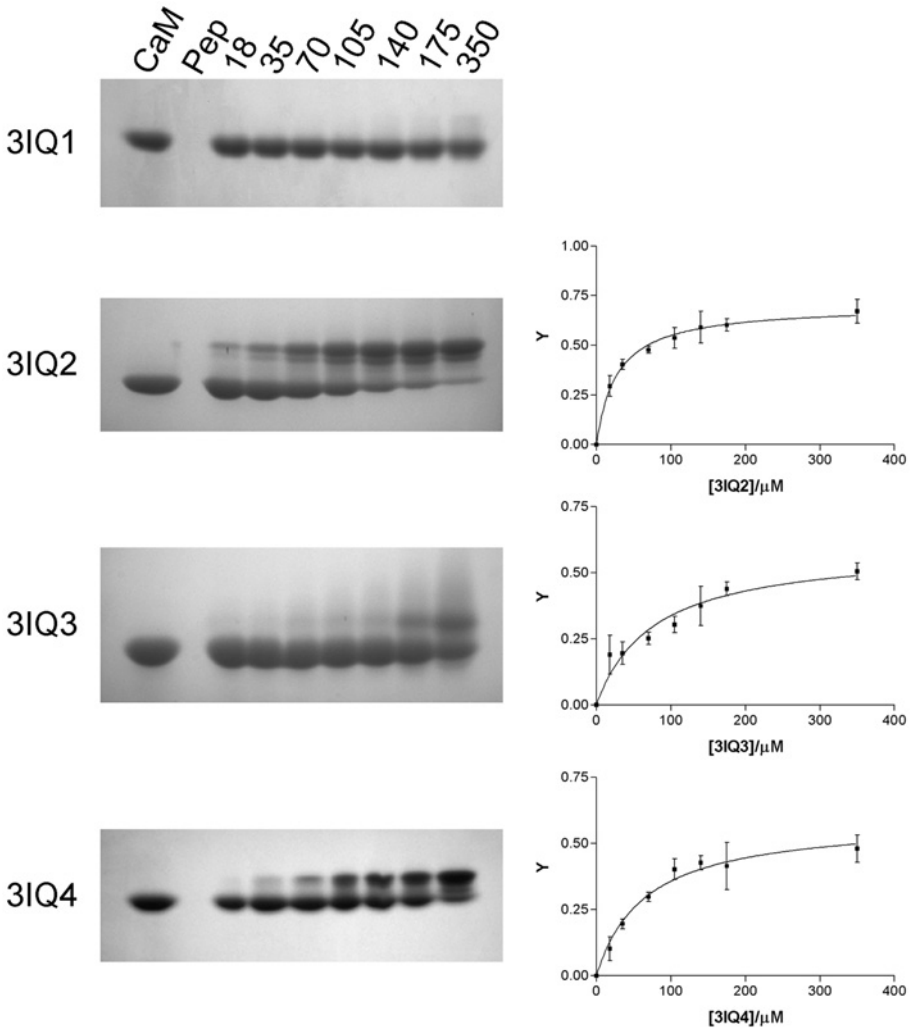


**Figure 4** **Interaction of IQ-motif peptides from IQGAP3 with CaM (35 $\mu$M)**

The left-hand panels show the gel shifts with the peptide concentrations given above in $\mu$M. CaM represents the calmodulin-only (35 $\mu$M) control and Pep the peptide-only (350 $\mu$M) control. The right-hand panels show graphs of the fraction bound ($Y$) against peptide concentration fitted to the binding equation $Y = Y_{max}[\text{peptide}]/K_{d,app} + [\text{peptide}]$. Each point represents the mean of three independent determinations (as described in the Materials and methods section) and the error bars the S.D. of these means. For each experiment, the goodness of fit was ascertained by comparing the fit to this equation with a fit to a straight line (*F*-test). In all cases, the better fit was to the binding equation. The quality of data was assessed by calculation of the residuals. In all cases, these were small and random.

## DISCUSSION

The results presented here show that there are clear differences in the affinity of the various IQ-motifs for CaM. Furthermore, they also demonstrate that there are (at least) two modes of interaction. Some IQ-motifs form complexes that are stable under the conditions of native gel electrophoresis. This method is a non-equilibrium technique. Prior to electrophoresis, there is an equilibrium between the bound and unbound material. Once the current is applied the bound and unbound begin to separate (since they have different masses and overall charges). This disturbs the equilibrium which will tend to reassert itself (Le Chatelier's Principle). The speed at which this occurs determines whether or not a discrete band will be observed. If dissociation of the complex is slow, with respect to the time of electrophoresis, then a discrete band will be observed representing a stable complex. If the dissociation time is comparable with the electrophoresis time, then blurring may be observed as the complex has partially dissociated during the experiment. These more dynamic complexes may be important in transducing transient changes in the prevailing calcium ion concentration, whereas the longer-lived complexes will remain bound if there are temporary reductions in the calcium concentration.

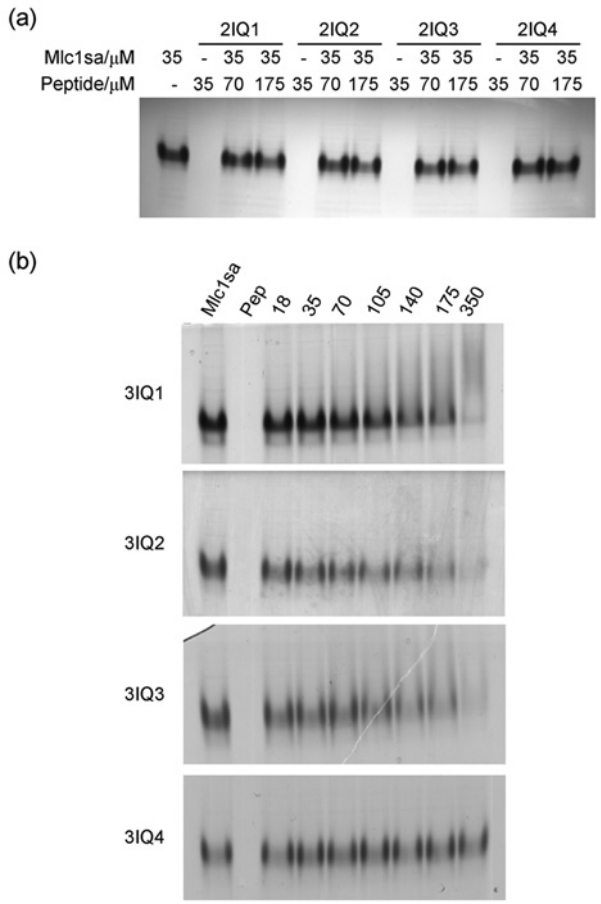


**Figure 5 Interaction between the IQ-motifs of IQGAP2 and IQGAP3 and the myosin essential light chain, Mlc1sa**

(a) No interactions were detected between the IQ-motifs of IQGAP2 and Mlc1sa (concentrations indicated above the gel). (b) The first IQ-motif from IQGAP3 interacts with Mlc1sa. This interaction shows a clear dependence of shift on peptide concentration, but does not result in a discrete band corresponding to the peptide–Mlc1sa complex. For the second and third IQ-motifs, some blurring of the protein band was observed. No interaction between the fourth IQ-motif and Mlc1sa was detected. The numbers above the gels indicate the peptide concentration in $\mu$M. Mlc1sa represents the myosin essential light chain-only (35 $\mu$M) control and Pep the peptide-only (35 $\mu$M) control. These results are representative of three independent experiments.

**Table 2 Interactions of IQ motifs from the three human isoforms of IQGAP1 with CaM and the structurally related proteins myosin essential light chain and S100B**

The IQ motifs for IQGAP1 are named in a similar manner to that used in the present paper for IQGAP2 and IQGAP3 (i.e. 1IQ1, etc., in the order they appear in the primary sequence). The lifetime of the complex has been assessed from whether or not discrete bands were observed on native gel electrophoresis. In [32], the main method for detecting interaction with CaM was CaM–Sepharose pull-downs. Since this is also a non-equilibrium technique, it can be assumed that these interactions are also relatively long-lived. It is likely that future experiments will expand the list of known binders.

| IQ-motif | Known binding | Reference |
|---|---|---|
| 1IQ1 | Mlc1sa (long-lived) | [35] |
| | S100B + $Ca^{2+}$ (long-lived) | [35] |
| | CaM + $Ca^{2+}$ | [32] |
| 1IQ2 | S100B + $Ca^{2+}$ (long-lived) | [35] |
| | CaM + $Ca^{2+}$ | [32] |
| 1IQ3 | CaM-$Ca^{2+}$ | [32] |
| | CaM + $Ca^{2+}$ | [32] |
| | Rap1* | [56] |
| 1IQ4 | CaM-$Ca^{2+}$ | [32] |
| | CaM + $Ca^{2+}$ | [32] |
| | Rap1 | [56] |
| 2IQ1 | CaM-$Ca^{2+}$ (transient) | This work |
| 2IQ2 | CaM + $Ca^{2+}$ (transient) | This work |
| 2IQ3 | CaM + $Ca^{2+}$ (intermediate lifetime) | This work |
| 2IQ4 | None detected | |
| 3IQ1 | CaM + $Ca^{2+}$ (transient) | This work |
| | CaM-$Ca^{2+}$ (transient)? | This work |
| | Mlc1sa (transient) | This work |
| 3IQ2 | CaM + $Ca^{2+}$ (long-lived) | This work |
| 3IQ3 | CaM + $Ca^{2+}$ (long-lived) | This work |
| 3IQ4 | CaM + $Ca^{2+}$ (long-lived) | This work |

*The binding of the GTPase Rap1 has been localized to both 1IQ3 and 1IQ4. It is possible that only one is required or that further sequences are needed for recognition and interaction.

The interaction of 3IQ1 with Mlc1sa was not unexpected since, of the eight IQ-motifs studied here, it is the most similar to the first IQ-motif from IQGAP1 (1IQ1). This motif, which shows similarity to myosin essential light chain binding regions in myosin heavy chains, has already been shown to interact with Mlc1sa [34,35]. However, the mode of interaction with the two IQ-motifs is different. Discrete shifts were observed with 1IQ1 [35], whereas less discrete, more blurred shifts were seen here (Figure 5). This may mean that IQGAP1 has long-lived, stable interactions with Mlc1sa while IQGAP3 makes more transient ones. However, in the absence of *in vivo* data on the significance of this interaction, the possibility of artefactual binding due to the high similarity to 1IQ1 cannot be ruled out completely. The physiological significance of the interaction between mammalian IQGAPs and myosin light chains is not clear. It has been suggested by analogy with yeasts that the interaction may be important in cytokinesis [52]. Although mammalian and sea urchin IQGAPs have been implicated in cytokinesis [26,53], thus far only the IQGAP–Cdc42 interaction has been shown to be important in this process.

Taking the data presented here together with previously published work, we can begin to understand the selectivity of the various IQ-motifs towards CaM and related proteins (Table 2). This suggests considerable differences between the three human isoforms. Interestingly, very little binding to the IQ-motifs from IQGAP2 was detected. It is possible that these motifs only interact with CaM very transiently (i.e. with half-lives of seconds or less) as such interactions would not be detected by this gel electrophoresis method. Previous work has suggested that the arginine residues of the motifs are important for the binding of CaM in the absence of calcium ions [32]. This is only partly supported

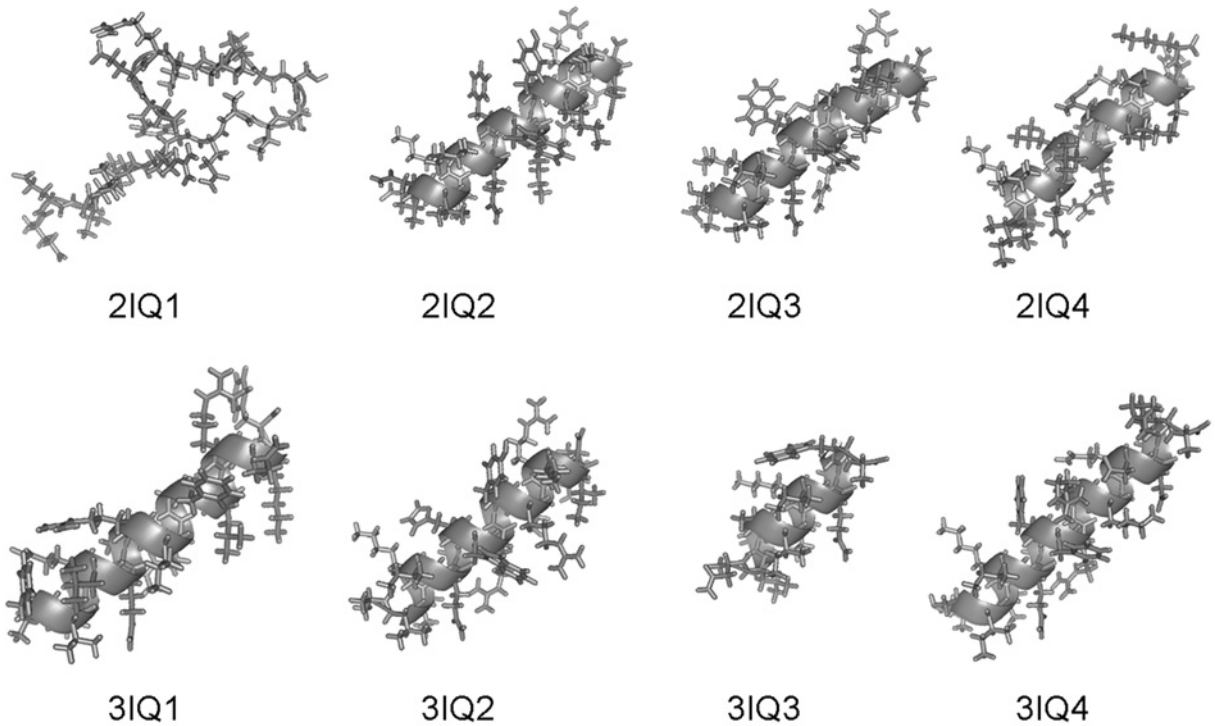


**Figure 6 Modelled structures of the IQ-motifs from human IQGAP2 and IQGAP3**
The peptide backbone is shown as a cartoon and the side chains in ball and stick format. In each case, the N-terminus of the peptide is in the lower left-hand corner of the structure. All except 2IQ2 display an $\alpha$-helical conformation. 2IQ2 has a random coil conformation with no recognizable elements of secondary structure. For clarity, the models are shown in the absence of solvating water molecules. 3IQ3 appears shorter than the remainder as only part of this sequence could modelled by the Phyre server. This may indicate that this motif has a more flexible or random coil structure than the other IQ-motifs from IQGAP3.

by the data presented here. While 3IQ1 has both arginine residues, 2IQ1 only has the second one (Figure 1). Unlike in IQGAP1, very little interaction between the IQ-motifs and CaM was detected in the absence of calcium ions with only 2IQ1 and, perhaps, 3IQ1 interacting under these conditions. Again this suggests differences between the three isoforms. Although the IQ-motifs from IQGAP2 and IQGAP3 may interact transiently in the absence of calcium (and thus not be detected by this method), interactions with IQGAP1 were also detected by non-equilibrium methods and must, therefore, be relatively long-lived [32,33].

The various IQ-motifs show some similarity and when the IQ-motifs from all three human IQGAP family proteins were compared, it was found that they tend to cluster according to position in sequence and not according to the protein from which they were derived – i.e. 1IQ1, 2IQ1 and 3IQ1 clustered together rather than all the motifs from IQGAP1, etc. clustering (Figure 7). Consistent with the molecular modelling data (Figure 6), 2IQ1 is the motif showing least similarity to the other 11. This lends support to the hypothesis that this motif has a different structure and, thus, may explain its ability to interact with CaM in the absence of calcium ions despite lacking one of the arginine residues. 2IQ1 is also the motif that is completely absent from the testicular splice variant of human IQGAP2 [28], suggesting that the signals transduced by this motif are not present in this tissue.

The interaction with CaM in the presence of calcium ions is believed to rely largely on non-polar interactions, with the first isoleucine residue being particularly important [32]. Again the results presented here partly support this conclusion. The three IQ-motifs that interact most stably with CaM in the presence of calcium ions (3IQ2, 3IQ3 and 3IQ4), all contain several non-polar residues including isoleucine. However, this is also the case for 2IQ2, 2IQ3 and 2IQ4 (which have no or transient interactions with CaM) suggesting that additional factors are important in determining which motifs can interact. Structural work suggests that substitution of the glycine residue of the IQ-motif with larger side chains results in a more extended conformation of the bound myosin light chain or CaM in myosin V [4]. If this logic is extended to IQGAP2 and IQGAP3, then Mlc1sa is bound in a compact formation to 3IQ1 and CaM binds in a compact formation, except to 2IQ3 and 3IQ3. These two IQ-motifs may interact with a more extended form of CaM. However, the cardiac $Ca_v1.2$ calcium channel the IQ-motif, which contains a bulky lysine residue in place of the glycine, binds to a compact form of calcium-CaM [54]. Overall, the work presented here extends our knowledge of

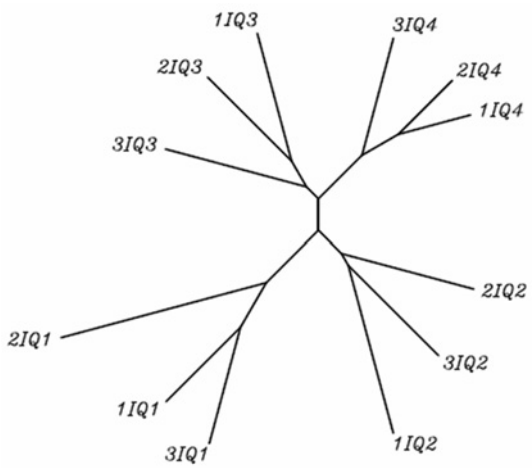


**Figure 7 The similarity of all 12 IQ-motifs from human IQGAP1, IQGAP2 and IQGAP3**

An alignment was generated using ClustalW (as implemented at http://align.genome.jp/) [55] applying the BLOSUM matrix for both pairwise and multiple alignments. The gap opening penalty was 10 and the gap extension penalty 0.1. The unrooted dendrogram based on that alignment is shown. Interestingly, the motifs group according to position in the primary sequence, not the isoform they are derived from. Consistent with its predicted random coil structure, 2IQ1 is the most distantly related motif.

how CaM interacts with the IQ-motifs of IQGAP family proteins and also highlights the need for high-resolution structural studies on these interactions.

## AUTHOR CONTRIBUTION

Erwan Atcheson and Elaine Hamilton carried out the CaM/IQ-motif and Mlc1sa/IQ-motif binding experiments respectively. Sevvel Pathmanthan developed the purification method for recombinant human CaM. Brett Greer and Pat Harriott synthesized the peptides. David Timson conceived the investigation, constructed the human CaM expression plasmid, carried out the modelling studies, supervised Erwan Atcheson, Elaine Hamilton and Sevvel Pathmanthan and wrote the initial draft of manuscript. All authors were involved in refining this manuscript and approved the final submitted version.

## ACKNOWLEDGEMENT

We thank Nadia Bouteldja for carrying out preliminary work on this project as part of a Biochemical Society funded summer studentship.

## FUNDING

This work was supported, in part, by the Biotechnology and Biological Sciences Research Council, U.K. [grant number BB/D000394/1]. E.A. thanks the Wellcome Trust, UK for a summer vacation studentship, E.H. thanks the Department of Employment and Learning, Northern Ireland and S.P. thanks Queen's University, Belfast for postgraduate research studentships.

## REFERENCES

1 Bahler, M. and Rhoads, A. (2002) Calmodulin signaling via the IQ motif. FEBS Lett. 513, 107–113
2 Cheney, R. E. and Mooseker, M. S. (1992) Unconventional myosins. Curr. Opin. Cell Biol. 4, 27–35
3 Wakim, B. T., Alexander, K. A., Masure, H. R., Cimler, B. M., Storm, D. R. and Walsh, K. A. (1987) Amino acid sequence of P-57, a neurospecific calmodulin-binding protein. Biochemistry 26, 7466–7470
4 Terrak, M., Rebowski, G., Lu, R. C., Grabarek, Z. and Dominguez, R. (2005) Structure of the light chain-binding domain of myosin V. Proc. Natl. Acad. Sci. U.S.A. 102, 12718–12723
5 Rayment, I., Rypniewski, W. R., Schmidt-Base, K., Smith, R., Tomchick, D. R., Benning, M. M., Winkelmann, D. A., Wesenberg, G. and Holden, H. M. (1993) Three-dimensional structure of myosin subfragment-1: a molecular motor. Science 261, 50–58
6 Hart, M. J., Callow, M. G., Souza, B. and Polakis, P. (1996) IQGAP1, a calmodulin-binding protein with a rasGAP-related domain, is a potential effector for cdc42Hs. EMBO J. 15, 2997–3005
7 Briggs, M. W. and Sacks, D. B. (2003) IQGAP proteins are integral components of cytoskeletal regulation. EMBO Rep. 4, 571–574
8 Ho, Y. D., Joyal, J. L., Li, Z. and Sacks, D. B. (1999) IQGAP1 integrates $Ca^{2+}$/calmodulin and Cdc42 signaling. J. Biol. Chem. 274, 464–470
9 Joyal, J. L., Annan, R. S., Ho, Y. D., Huddleston, M. E., Carr, S. A., Hart, M. J. and Sacks, D. B. (1997) Calmodulin modulates the interaction between IQGAP1 and Cdc42identification of IQGAP1 by nanoelectrospray tandem mass spectrometry. J. Biol. Chem. 272, 15419–15425
10 Erickson, J. W., Cerione, R. A. and Hart, M. J. (1997) Identification of an actin cytoskeletal complex that includes IQGAP and the Cdc42 GTPase. J. Biol. Chem. 272, 24443–24447
11 Brown, M. D. and Sacks, D. B. (2006) IQGAP1 in cellular signaling: Bridging the GAP. Trends Cell Biol. 16, 242–249
12 Weissbach, L., Settleman, J., Kalady, M. F., Snijders, A. J., Murthy, A. E., Yan, Y. X. and Bernards, A. (1994) Identification of a human rasGAP-related protein containing calmodulin-binding motifs. J. Biol. Chem. 269, 20517–20521
13 Bashour, A. M., Fullerton, A. T., Hart, M. J. and Bloom, G. S. (1997) IQGAP1, a rac- and Cdc42-binding protein, directly binds and cross-links microfilaments. J. Cell Biol. 137, 1555–1566
14 Le Clainche, C., Schlaepfer, D., Ferrari, A., Klingauf, M., Grohmanova, K., Veligodskiy, A., Didry, D., Le, D., Egile, C., Carlier, M. F. and Kroschewski, R. (2007) IQGAP1 stimulates actin assembly through the N-WASP-Arp2/3 pathway. J. Biol. Chem. 282, 426–435
15 Fukata, M., Watanabe, T., Noritake, J., Nakagawa, M., Yamaga, M., Kuroda, S., Matsuura, Y., Iwamatsu, A., Perez, F. and Kaibuchi, K. (2002) Rac1 and Cdc42 capture microtubules through IQGAP1 and CLIP-170. Cell 109, 873–885
16 Watanabe, T., Wang, S., Noritake, J., Sato, K., Fukata, M., Takefuji, M., Nakagawa, M., Izumi, N., Akiyama, T. and Kaibuchi, K. (2004) Interaction with IQGAP1 links APC to Rac1, Cdc42, and actin filaments during cell polarization and migration. Dev. Cell 7, 871–883
17 Mateer, S. C., McDaniel, A. E., Nicolas, V., Habermacher, G. M., Lin, M. J., Cromer, D. A., King, M. E. and Bloom, G. S. (2002) The mechanism for regulation of the F-actin binding activity of IQGAP1 by calcium/calmodulin. J. Biol. Chem. 277, 12324–12333
18 Mateer, S. C., Morris, L. E., Cromer, D. A., Bensenor, L. B. and Bloom, G. S. (2004) Actin filament binding by a monomeric IQGAP1 fragment with a single calponin homology domain. Cell Motil. Cytoskeleton 58, 231–241
19 Osman, M. A. and Cerione, R. A. (1998) Iqg1p, a yeast homologue of the mammalian IQGAPs, mediates cdc42p effects on the actin cytoskeleton. J. Cell Biol. 142, 443–455

20 Shannon, K. B. and Li, R. (1999) The multiple roles of Cyk1p in the assembly and function of the actomyosin ring in budding yeast. Mol. Biol. Cell 10, 283–296
21 Swart-Mataraza, J. M., Li, Z. and Sacks, D. B. (2002) IQGAP1 is a component of Cdc42 signaling to the cytoskeleton. J. Biol. Chem. 277, 24753–24763
22 Brill, S., Li, S., Lyman, C. W., Church, D. M., Wasmuth, J. J., Weissbach, L., Bernards, A. and Snijders, A. J. (1996) The ras GTPase-activating-protein-related human protein IQGAP2 harbors a potential actin binding domain and interacts with calmodulin and rho family GTPases. Mol. Cell. Biol. 16, 4869–4878
23 Mataraza, J. M., Briggs, M. W., Li, Z., Frank, R. and Sacks, D. B. (2003) Identification and characterization of the Cdc42-binding site of IQGAP1. Biochem. Biophys. Res. Commun. 305, 315–321
24 Pathmanathan, S., Barnard, E. and Timson, D. J. (2008) Interactions between the budding yeast IQGAP homologue Iqg1p and its targets revealed by a split-EGFP bimolecular fluorescence complementation assay. Cell Biol. Int. 32, 1318–1322
25 Sokol, S. Y., Li, Z. and Sacks, D. B. (2001) The effect of IQGAP1 on *Xenopus* embryonic ectoderm requires Cdc42. J. Biol. Chem. 276, 48425–48430
26 Nishimura, Y. and Mabuchi, I. (2003) An IQGAP-like protein is involved in actin assembly together with Cdc42 in the sea urchin egg. Cell Motil. Cytoskeleton. 56, 207–218
27 Bernards, A. (2003) GAPs galore! A survey of putative ras superfamily GTPase activating proteins in man and *Drosophila*. Biochim. Biophys. Acta 1603, 47–82
28 Wang, H., Huo, R., Xu, M., Lu, L., Xu, Z., Li, J., Zhou, Z. and Sha, J. (2004) Cloning and characterization of a novel transcript variant of IQGAP2 in human testis. DNA Seq. 15, 319–325
29 Wendland, J. and Philippsen, P. (2002) An IQGAP-related protein, encoded by AgCYK1, is required for septation in the filamentous fungus *Ashbya gossypii*. Fungal Genet. Biol. 37, 81–88
30 Boyne, J. R., Yosuf, H. M., Bieganowski, P., Brenner, C. and Price, C. (2000) Yeast myosin light chain, Mlc1p, interacts with both IQGAP and class II myosin to effect cytokinesis. J. Cell Sci. 113, 4533–4543
31 Lippincott, J. and Li, R. (1998) Sequential assembly of myosin II, an IQGAP-like protein, and filamentous actin to a ring structure involved in budding yeast cytokinesis. J. Cell Biol. 140, 355–366
32 Li, Z. and Sacks, D. B. (2003) Elucidation of the interaction of calmodulin with the IQ motifs of IQGAP1. J. Biol. Chem. 278, 4347–4352
33 Li, Q. and Stuenkel, E. L. (2004) Calcium negatively modulates calmodulin interaction with IQGAP1. Biochem. Biophys. Res. Commun. 317, 787–795
34 Weissbach, L., Bernards, A. and Herion, D. W. (1998) Binding of myosin essential light chain to the cytoskeleton-associated protein IQGAP1. Biochem. Biophys. Res. Commun. 251, 269–276
35 Pathmanathan, S., Elliott, S. F., McSwiggen, S., Greer, B., Harriott, P., Irvine, G. B. and Timson, D. J. (2008) IQ motif selectivity in human IQGAP1: Binding of myosin essential light chain and S100B. Mol. Cell. Biochem. 318, 43–51
36 D'souza, V. M., Naqvi, N. I., Wang, H. and Balasubramanian, M. K. (2001) Interactions of Cdc4p, a myosin light chain, with IQ-domain containing proteins in *Schizosaccharomyces pombe*. Cell Struct. Funct. 26, 555–565
37 Shannon, K. B. and Li, R. (2000) A myosin light chain mediates the localization of the budding yeast IQGAP-like protein during contractile ring formation. Curr. Biol. 10, 727–730
38 Korinek, W. S., Bi, E., Epp, J. A., Wang, L., Ho, J. and Chant, J. (2000) Cyk3, a novel SH3-domain protein, affects cytokinesis in yeast. Curr. Biol. 10, 947–950
39 Corbett, M., Xiong, Y., Boyne, J. R., Wright, D. J., Munro, E. and Price, C. (2006) IQGAP and mitotic exit network (MEN) proteins are required for cytokinesis and re-polarization of the actin cytoskeleton in the budding yeast, *Saccharomyces cerevisiae*. Eur. J. Cell Biol. 85, 1201–1215
40 Osman, M. A., Konopka, J. B. and Cerione, R. A. (2002) Iqg1p links spatial and secretion landmarks to polarity and cytokinesis. J. Cell Biol. 159, 601–611
41 Li, C. R., Wang, Y. M. and Wang, Y. (2008) The IQGAP Iqg1 is a regulatory target of CDK for cytokinesis in *Candida albicans*. EMBO J. 27, 2998–3010
42 Eng, K., Naqvi, N. I., Wong, K. C. and Balasubramanian, M. K. (1998) Rng2p, a protein required for cytokinesis in fission yeast, is a component of the actomyosin ring and the spindle pole body. Curr. Biol. 8, 611–621
43 Wu, J. Q., Sirotkin, V., Kovar, D. R., Lord, M., Beltzner, C. C., Kuhn, J. R. and Pollard, T. D. (2006) Assembly of the cytokinetic contractile ring from a broad band of nodes in fission yeast. J. Cell Biol. 174, 391–402
44 Mbele, G. O., Deloulme, J. C., Gentil, B. J., Delphin, C., Ferro, M., Garin, J., Takahashi, M. and Baudier, J. (2002) The zinc- and calcium-binding S100B interacts and co-localizes with IQGAP1 during dynamic rearrangement of cell membranes. J. Biol. Chem. 277, 49998–50007
45 Lennon, G., Auffray, C., Polymeropoulos, M. and Soares, M. B. (1996) The I.M.A.G.E. consortium: An integrated molecular analysis of genomes and their expression. Genomics. 33, 151–152
46 Bradford, M. M. (1976) A rapid and sensitive method for the quantitation of microgram quantities of protein utilizing the principle of protein-dye binding. Anal. Biochem. 72, 248–254
47 Fields, G. B. and Noble, R. L. (1990) Solid phase peptide synthesis utilizing 9-fluorenylmethoxycarbonyl amino acids. Int. J. Pept. Protein Res. 35, 161–214
48 Marquardt, D. (1963) An algorithm for least squares estimation of nonlinear parameters. SIAM J. Appl. Math. 11, 431–441
49 Kelley, L. A. and Sternberg, M. J. (2009) Protein structure prediction on the web: a case study using the phyre server. Nat. Protoc. 4, 363–371
50 Krieger, E., Joo, K., Lee, J., Lee, J., Raman, S., Thompson, J., Tyka, M., Baker, D. and Karplus, K. (2009) Improving physical realism, stereochemistry, and side-chain accuracy in homology modeling: Four approaches that performed well in CASP8. Proteins 77 (Suppl. 9), 114–122
51 Gopalakrishna, R. and Anderson, W. B. (1982) $Ca^{2+}$-induced hydrophobic site on calmodulin: application for purification of calmodulin by phenyl-Sepharose affinity chromatography. Biochem. Biophys. Res. Commun. 104, 830–836
52 Timson, D. J. (2010) The IQGAP-myosin light chain interaction: what is its function? In Cytoskeleton: Cell Movement, Cytokinesis and Organelles Organization (Lansing, S. and Rosseau, T., eds), pp. 139–147, Nova Science Publishers, New York
53 Bielak-Zmijewska, A., Kolano, A., Szczepanska, K., Maleszewski, M. and Borsuk, E. (2008) Cdc42 protein acts upstream of IQGAP1 and regulates cytokinesis in mouse oocytes and embryos. Dev. Biol. 322, 21–32
54 Fallon, J. L., Halling, D. B., Hamilton, S. L. and Quiocho, F. A. (2005) Structure of calmodulin bound to the hydrophobic IQ domain of the cardiac $Ca_v1.2$ calcium channel. Structure 13, 1881–1886
55 Chenna, R., Sugawara, H., Koike, T., Lopez, R., Gibson, T. J., Higgins, D. G. and Thompson, J. D. (2003) Multiple sequence alignment with the clustal series of programs. Nucleic Acids Res. 31, 3497–3500
56 Jeong, H. W., Li, Z., Brown, M. D. and Sacks, D. B. (2007) IQGAP1 binds Rap1 and modulates its activity. J. Biol. Chem. 282, 20752–20762

**Received 2 November 2010/16 December 2010; accepted 8 February 2011**
**Published as Immediate Publication 8 February 2011, doi 10.1042/BSR20100123**

Biosci. Rep. (2011) / **31** / 371–379 (Printed in Great Britain) / doi 10.1042/BSR20100123

online data

multimedia

Original Paper

## SUPPLEMENTARY ONLINE DATA

# IQ-motif selectivity in human IQGAP2 and IQGAP3: binding of calmodulin and myosin essential light chain

Erwan ATCHESON, Elaine HAMILTON[1], Sevvel PATHMANATHAN[2], Brett GREER, Pat HARRIOTT and David J. TIMSON[3]

School of Biological Sciences, Queen's University Belfast, Medical Biology Centre, 97 Lisburn Road, Belfast BT9 7BL. U.K.

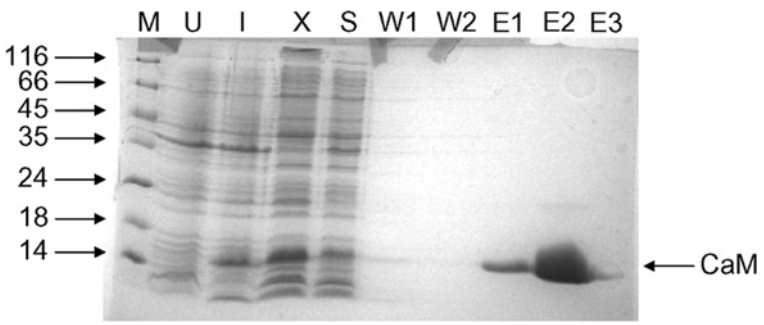


**Figure S1 Purification of recombinant human CaM**

M, molecular mass markers (sizes indicated to the left in kDa); U, extract from uninduced cells prior to induction; I, extract from cells 2 h after induction with 2 mM IPTG; X, extract following sonication; S, soluble material following centrifugation, prior to loading on to the phenyl Sepharose column; W1 and W2, material passing through the column during washing; E1, E2 and E3, elutions. The majority of the purified protein appears in the second elution (indicated by an arrow to the right of the gel).

**Received 2 November 2010/16 December 2010; accepted 8 February 2011**
**Published as Immediate Publication 8 February 2011, doi 10.1042/BSR20100123**

[1]Present address: Belfast Metropolitan College, Castlereagh Campus, Montgomery Road, Belfast BT6 9JD, U.K.
[2]Present address: Department of Botany, The University of Jaffna, Jaffna, Sri Lanka.
[3]To whom correspondence should be addressed (email d.timson@qub.ac.uk).